Environ Monit Assess (2018) 190: 647
https://doi.org/10.1007/s10661-018-7026-3

Distribution and isotopic signature of deep gases in submerged soils in an island of the Lower Delta of the Paraná River, Argentina

Romina Sanci · Héctor Osvaldo Panarello

Received: 20 April 2018 / Accepted: 2 October 2018 / Published online: 18 October 2018

Abstract Subsoil CH_4 and CO_2 concentrations, δ^{13}C-CH_4 and δ^{13}C-CO_2 signatures, total organic carbon (TOC) and δ^{13}C-TOC, together with C/N ratio of organic matter, were evaluated throughout a soil profile up to the atmosphere to understand the dynamics of CH_4 and CO_2 in the waterlogged environment of an island of the Lower Delta of the Paraná River, Argentina. The analysis of the vertical profile showed that a significant fraction of CH_4 exists as gas trapped within the sediment column, compared to CH_4 dissolved in soil solution. CH_4 concentration measurements in sub-saturated soils showed that free CH_4 is 1 order of magnitude smaller than CH_4 recovered from soil cores by ultrasonic degassing. The highest concentrations of CH_4 occurred at the 90–120-cm layer. At this depth, δ^{13}C-CH_4 values resulting from methanogenesis were around − 71‰, which is well within the range of CH_4 produced from CO_2 reduction, and δ^{13}C values of the associated CO_2 were enriched (~ − 7‰). Isotope mass balance models used to calculate the fraction of oxidized CH_4 indicated that around 30% of the CH_4 produced was oxidized prior to atmospheric release. In contrast to methanogenesis, during oxidation processes δ^{13}C-CH_4 shifts to more positive values. The mineralogical, textural, isotopic, and geochemical characterization of subsoil sediments with abundant organic matter, like Paraná Delta, demonstrated that CH_4 storage capacity of the soil, production, consumption, and transport are the main factors in regulating the actual flux rates of CH_4 to the atmosphere.

Keywords CH_4 pools · Deep gases · C isotope tracer · Wetland

R. Sanci (✉)
Instituto de Geociencias Básicas, Aplicadas y Ambientales de Buenos Aires (IGEBA), Intendente Güiraldes 2160, Pabellón II, Piso 1, CP 1428 Ciudad Universitaria, CABA, Argentina
e-mail: rominasanci@gmail.com

H. O. Panarello
Instituto de Geocronología y Geología Isotópica, Intendente Güiraldes 2160, Pabellón INGEIS, CP 1428 Ciudad Universitaria, CABA, Argentina
e-mail: hpanarello@yahoo.com.ar

Introduction

Wetlands contribute as much as 70% of the total natural CH_4 emissions (Khalil 2000; Wuebbles and Hayhoe 2002). These sites are characterized by an anaerobic zone of CH_4 production and by submerged or water-saturated soils with a high content of organic matter. In these environments, CH_4 is generated from the terminal fermentation products of organic matter by methanogenic archaea and it is typically found at depths greater than the soil-atmosphere interface. CH_4 emissions from most types of wetlands, such as marshes, swamps, bogs, and fens (EPA 2001), can vary by several orders of magnitude over just a few meters, because they are influenced by a wide range of environmental parameters. These parameters include soil characteristics, such as the availability of organic carbon and nutrients, plant physiology, community composition, cover, water table depth, and soil temperature. Some authors state that once the anaerobic conditions for the production of

CH_4 are reached, the quality and supply of substrates is the main factor that regulates its production (Hornibrook et al. 1997; Chanton 2005). Nevertheless, CH_4 released from soils is only a fraction of the total CH_4 production because the CH_4 locally produced is retained in the soil and/or oxidized by aerobic methanotrophic bacteria in the rhizosphere and in surficial oxic layers during diffusive transport to the soil surface (Whalen 2005; Bridgham et al. 2013). Research on CH_4 capture and degassing from saturated sediments of different sources, such as rice fields (Wassmann et al. 1996), wetlands (i.e., Chanton et al. 1989; Baird et al. 2004; Strack et al. 2004), permafrost soils (Preuss et al. 2013), and seafloor sediments (Gal'chenko et al. 2004), shows that total CH_4 includes dissolved CH_4 and CH_4 sorbed in the mineral and/or aqueous components of the sediments. Thus, specific studies about internal carbon dynamics of wetlands not only focus on monitoring surface emissions of both CH_4 and CO_2 and spatial variability (e.g., Couwenberg et al. 2010; Kayranli et al. 2010), but also on the dissolution of these deep gases within the profile (e.g., Waldron et al. 1999; Steinmann et al. 2008; Garnett et al. 2011) and the mechanisms that regulate their accumulation (e.g., Comas et al. 2005, 2014; Ramirez et al. 2015).

Studies about gases in wetlands-peatlands (e.g., Aravena et al. 1993; Le Mer and Roger 2001; Glaser et al. 2004; Strack et al. 2005; Rosenberry et al. 2006; Coulthard et al. 2009; Lai 2009) have shown that CH_4 concentrations are the result of the balance between production, consumption (oxidation), migration, and storage mechanisms. This balance, and, thus, the net fluxes to the atmosphere from individual wetland environments, can be studied through the isotopic values of CH_4 (Whiticar 1999; Chanton 2005; Conrad 2005). Moreover, isotopic fractionation of C during CH_4 production and consumption, as well as isotopic differences in organic carbon sources, defines the isotopic value of the net flux from a specific site (Martens et al. 1992).

In Argentina, there are places where CH_4 and CO_2 are produced in a natural way. An example is the so-called marsh gas in the Delta of the Paraná River, which was historically used by some local people as a source of renewable energy for cooking and lighting. The mouth of the Paraná River in the Río de la Plata generates a bayhead delta, of the same name, with a typical aggradation and progradation structure that is characterized by having large channels with well-developed levees constituted by silty-sandy to fine sandy sediments, enclosing central depressions occupied by permanent or semipermanent lagoons (Medina and Codignotto 2013). The periodic floods of these sectors give this region the characteristics of a fluvio-coastal wetland (Malvárez 1997). It is precisely in these topographically depressed areas with accumulation of plant organic matter and frequent waterlogging (without oxygen availability) where reducing conditions are generated for the formation of CH_4 (and associated CO_2) at high concentrations. Despite the knowledge of the existence of this resource in the islands, nowadays its use is isolated and sporadic, since the massive provision of gas or fuel is through gas cylinders. Thus, the processes involved in the CH_4 production in deeper layers, below the first centimeters of soil in the Paraná Delta, have not been well studied. In order to study these deep gases, we carried out a research in one of the islands. We used chemical and isotopic data to characterize the surface and deep processes in a quantitative way (emission through soil-atmosphere interface, production, oxidation, transport, and dissolution). $\delta^{13}C$ values of CH_4 and CO_2 were used to differentiate between types of methanogenesis in continuous subsoil layers below surface and to estimate transported/oxidized CH_4 fractions. CH_4 and CO_2 concentrations, $\delta^{13}CH_4$ and $\delta^{13}CO_2$ signatures, total organic carbon (TOC) and $\delta^{13}C$-TOC, together with C/N ratio of organic matter were measured along the soil profile up to the atmosphere to understand the dynamics of CH_4 and CO_2 in this waterlogged environment. We chose a site of an island where people used the gases extracted from a drilling for domestic purposes, assuming that CH_4-CO_2 gases would be present in high concentrations.

Methods

Field work

Our study area is a private land of 60 m by 120 m located in an island of the Lower Parana Delta, between the Arroyón and Sábalos streams (Fig. 1), and stretching from the levee towards the center of the island. Years ago, there was a "homemade" drilling (now blocked), which allowed the locals to accumulate the gas on the surface and take it into the house for cooking and lighting uses. The soils in this zone were described as hydromorphic soils (INTA 1990). The Lower Delta is the terminal area of the so-called Paraná Delta, which

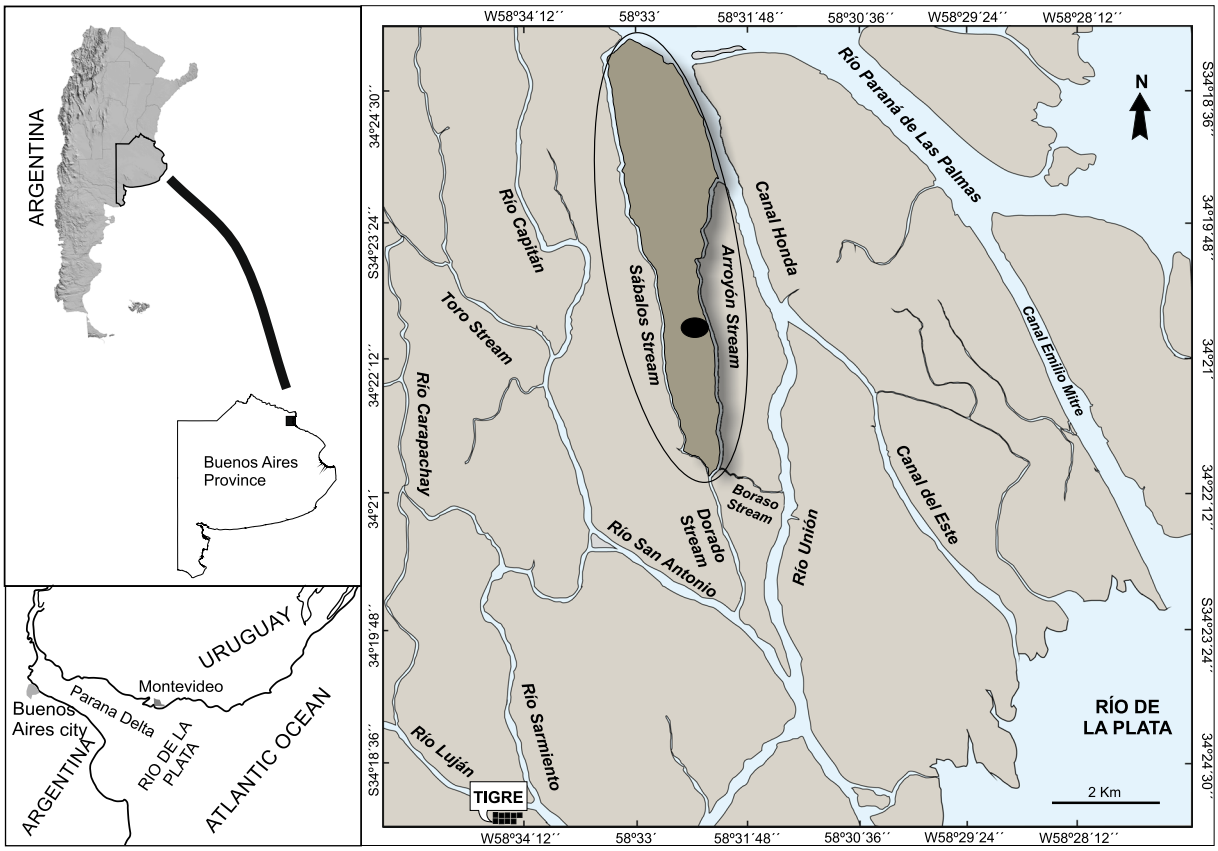

Fig. 1 Location map showing the study area (black circle). The sampling stations are placed inside of an island of the Lower Parana Delta, between the Arroyón and Sábalos streams

stretches across the final 300 km of the Paraná basin. This delta is one of the largest coastal wetlands systems of Argentina, spreading over 320 km and covering a surface of ~ 17,500 km^2 (Malvarez 1997). It is located between 32° 05′ S and 58° 30′ W, to the south of Diamante City (Entre Ríos), and between 34° 29′ S and 60° 48′ W in the surroundings of Buenos Aires City (Kandus et al. 2006). Since our previous experience had been with gases of non-saturated soils (Sanci et al. 2012; Sanci and Panarello 2016), experimental developments were needed in order to capture CH_4 and CO_2 from deep submerged soils. Based on bibliography about CH_4 entrapped in cores, we tested different techniques to extract and quantify these gases and its stable isotopic composition.

Three field trips were made during 2014 and 2015. In the first field trip, near-surface (< 4 cm) CH_4 concentrations were measured along several transects defined across the whole study area in order to obtain a semi-quantitative estimation of CH_4 concentration and detect the occurrence of gas anomalies. Measurements were carried out using a Photovac MicroFID analyzer with an accuracy of 0.1 ppmv, which operates in a range of 0.1 ppm to 1000 ppmv. Towards the center of the island, where a surface anomaly was found, we took soil cores from two depths (0–30 and 30–60 cm) with a hand held acrylic core of 30 cm long. Core samplers were sealed with a rubber stopper in order to minimize gas loss and ^{13}C air contamination. The cores were then stored in ice in the field until laboratory analysis. Moreover, disturbed soil samples were obtained with a hand probe every 20 cm up to a depth of 1.20 m to study soil characteristics related to gas production and accumulation. Three sampling points with different moisture conditions and land elevation were chosen: site A, right beside the levee; site B, halfway between sites A and C; and site C, towards the center of the island.

In the second field trip, we focused on quantifying surface emissions and total subsoil CH_4 (sorbed, free, and dissolved fractions) in the center of the island (Site

C), area where the anomalies had been detected. Subsurface gas traps (cores and bags) and pore-water samplers were used to measure subsurface CH_4 pools. Taking into account the experience of the first field trip, a new device for collecting soil cores and capture the subsoil gases (sorbed and free) was constructed. It consisted of acrylic tubes, 27 cm high and 6.3 cm diameter with extensible bars to reach different levels (30, 60, 90, 120 cm). The top of the tube was sealed and had a "Quick Connect Pressure Washer Adapter" joined to a 3/8″ Tygon hose which allowed attaching the device to a sampling Tedlar bag. The open end of the core was pushed vertically into the submerged soil, and the gas sampling bag was gradually filled with gases from the inner volume. Thus, emerging gases (or free gases) from each level were collected in these gas bags. When the core was detached from subsoil, the base was sealed with a rubber stopper, for later laboratory analysis. We extracted three complete cores very close to each other. Disturbed soil samples were also extracted at each level to measure total organic carbon and its ^{13}C composition. Dissolved CH_4 in the soil solution was sampled through macrorhizons® samplers containing a porous material with a pore size of ~ 0.18 μm. These samplers were fixed on a PVC frame allowing the collection of soil solution samples at different depths of the column by connecting a pre-evacuated glass tube.

CH_4 and CO_2 surface fluxes were determined using the technique known as the closed-chamber method, consisting in the determination of the rate of increase in the CH_4-CO_2 concentrations within a chamber placed on the soil surface. Measurements were carried out along four W-E transects, 20 m apart. Closed chambers were located on seven stations along these transects, every 20 m, thus creating a regular sampling grid over the experimental site.

A closed dynamic chamber was used to measure CO_2 fluxes. It consisted of a circular chamber (78 cm^2 of area and a volume of 1.17 L) with a rim and an interior fan, connected to an infrared analyzer (SRC-1 soil respiration chamber with IRGA PP Systems EGM-4). The detection range of CO_2 concentration was 0 to 30,000 μmol/mol. The chamber rim was inserted into the ground in order to eliminate the input of atmospheric air, which could cause significant errors, especially in windy days. The fan operated in order to improve gas mixing inside the chamber. The gas was continuously extracted, sent to the IRGA, and then reinjected into the chamber. CO_2 flux was determined using the rate of increase of CO_2 concentration, following the equation:

$$F \sim \frac{dC}{dt} \cdot \frac{V}{A}$$

The closed static chamber technique was used to estimate CH_4 fluxes. A chamber (450 cm^2 of area and a volume of 7.65 L) connected to the portable analyzer Madur GA21 Plus (measurement range between 0.01 and 4.95%) was placed on the ground to accumulate the CH_4 and the CH_4 gas soil concentration was recorded through time, according to Eq. (1). For C isotope measurements, gas samples were collected from this chamber through a capillary tube to avoid sudden pressure changes inside. Gas was extracted with a syringe and stored in glass vacuum flasks for laboratory isotope analysis.

In the third field trip, we repeated the closed chamber measurements, and soil core and disturbed soil sampling, but this time, on the three sites (A, B, and C).

Laboratory methods

Disturbed soil samples were analyzed for soil physicochemical and mineralogical characterization. Soil color was classified in wet and dry conditions (Munsell Soil Color Chart) and the texture of the samples was determined using the gravimetric method. The loss-on-ignition (LOI) method was used for the determination of organic matter which involves the heated destruction of all organic matter in the soil or sediment (Schumacher 2002). The soil moisture content was determined by drying the soil samples to constant weight and measuring the soil sample mass after and before drying (gravimetric method). Soil samples were analyzed for carbon and nitrogen isotopic and elemental composition at INGEIS laboratory. Given the relatively low content of organic matter, ca. 8 mg samples were loaded in tin capsules. Samples were measured in an elemental analyzer (Carlo Erba EA1108) coupled to a continuous flow isotope ratio mass spectrometer (Thermo Scientific Delta V Advantage), using a ConFlo IV interface. CO_2 obtained was diluted 80% via the ConFlo IV interface. To normalize the ^{13}C results, samples were measured together with internal references calibrated using the international standards L-SVEC, NBS-19, and NBS-22. $\delta^{13}C$ values were normalized on the L-SVEC-NBS-19 scale, according to Coplen et al. (2006) and have an uncertainty of ± 0.2‰. The nitrogen content of the samples proved to be insufficient for isotopic

measurement. The C/N ratio reported here is the atomic ratio, calculated from the carbon and nitrogen amount as % given by the EA-IRMS.

XRD was performed with a Bruker D2 PHASER equipment, CuKα radiation, scintillation counter detector at 30 kW and 15 mA. The samples were dried at 40 °C. For whole rock analysis, random samples were scanned between 3 and 70° 2θ, at 1° 2θ/min speed, with a step scan of 0.04° 2θ. Clay minerals were determined on the fraction < 2 μm obtained from suspensions by Stokes law and mounted as and oriented aggregate on glass slides. Scans from 2 to 30 2° θ were obtained on dry, overnight ethylene-glycol solvated samples, and after heating at 550 °C. For quantitative whole rock analysis, a Siroquant software was used. Clay minerals proportions were calculated following Biscaye (1965).

Sealed core samples, which contained a small gas headspace, were treated to release the trapped CH_4 within 24 h using two experimental procedures: shaking and ultrasonic energy. The shaking technique has been successfully applied to increase the CH_4 retrieval present in soil sediments (Bernard et al. 1978; Scranton et al. 1995; Wassmann et al. 1996), using different shaking times (10 min, 1 h, 10–12 h). In our case, core samples were vigorously shaken during 10, 20, 30, and 60 min. The ultrasonic procedure, during which cavitation reduces surface tension allowing the sorbed molecules to escape, allowed us to recover the CH_4 in less time. Ultrasonic energy was applied on cores for intervals of only a few seconds during a maximum time of 5 min to prevent possible chemical reactions of dissolved gases or oxidation (Schmitt et al. 1991). Nevertheless, taking into account that isotopic fractionation of the extracted CH_4 is possible during desorption processes (Magen et al. 2014), for interpretation purposes, we used the isotopic data from the tedlar bags. The gas released into the headspace of each core was extracted with a syringe and injected into pre-evacuated glass flasks sealed with butyl rubber.

CH_4 and CO_2 concentrations of gas samples were measured in a gas chromatography (GC) HP 5890 Series II with a thermal conductivity detector (TCD), a flame ionization detector (FID), and the analyzer Madur GA21 Plus. $^{13}C/^{12}C$ ratios were obtained using a GC-C-IRMS (TRACE GC Ultra, GC Isolink, ConFlo IV, Delta V Advantage). Samples were injected in splitless mode, using a 1-mL loop. Samples were cryo-trapped at the head of the GC column (Varian PoraPLOT Q 25 × 0.32) to improve peak shape. The delta values were calculated against the working standard, whose value was defined during the days before and after the GC measurements using the calibrated internal references of the EA coupled to the same IRMS. Data were reported as isotopic deviations (δ ‰) relative to the international reference standard Vienna Pee Dee Belemnite (V-PDB), with an uncertainty of ± 0.5‰ for both CH_4 and CO_2. Minimal sample requirement for GC-C-IRMS-^{13}C on CO_2 is ca. 1 μmol. Isotopic results were expressed as δ (‰), defined as:

$$\delta^{13}C = \frac{\left(^{13}C/^{12}C\right)_{sample} - \left(^{13}C/^{12}C\right)_{VPDB}}{\left(^{13}C/^{12}C\right)_{VPDB}} \times 10^3$$

where $\delta^{13}C$ is the isotopic deviation in ‰.

The concentration of CH_4 dissolved in water was determined by headspace equilibration and subsequent analysis by gas chromatography. The amount of gas dissolved in the sample was calculated using Henry's law. Sixty milliliters of ultra-pure helium was added, generating a headspace, allowing the system to equilibrate for an hour at room temperature. An aliquot of the headspace was analyzed with a gas chromatograph equipped with a Perkin Elmer Agilent 6890 elite-alumina, capillary column 50 m × 0.53 mm, and FID detector.

In order to verify the performance and reliability of the closed dynamic chamber, known CO_2 fluxes were imposed through an "artificial soil." The calibration system consisted of a container (30 cm of diameter), an accumulation chamber linked to the portable infrared gas analyzer, a flowmeter, and a calibrated gas cylinder containing CO_2 of known concentration. A 10-cm-thick layer of sand was placed at the top of the container supported by a wood disk homogeneously perforated, with an open mesh cloth to support the material. Pure CO_2 with known concentration was injected at the base of the container and the supply was regulated by a gas flowmeter. This gas flowed through the sand, simulating CO_2 diffusion through the soil. This system allowed determining the reliable range of CO_2 flux measurements. The chamber calibration results deviated from the imposed CO_2 flux values in 15% or less, while the reproducibility was better than 10%. Reliable CO_2 fluxes values were obtained in the range of 1.68 to 779.76 g/m^2 d.

Isotopic approach

During methanogenesis, CH_4 is enriched in the lighter carbon isotope (^{12}C) and the CO_2 associated with microbial CH_4 production is enriched in the heavier

isotope (^{13}C). Thus in an anoxic environment, such as a wetland, the $\delta^{13}C$-CO_2 is strongly affected by methanogenic reactions with reported values between − 10 and + 20‰. The $\delta^{13}C$ values of the different biogenic CH_4 pathways are generally known: CH_4 produced by acetate fermentation is not as depleted in ^{13}C as CH_4 produced from CO_2 reduction with H_2, with an isotopic composition ranging from − 65 to − 50‰ and − 110 to − 60‰, respectively (Whiticar et al. 1986). For example, in shallow soils containing abundant labile organic carbon, CH_4 production occurs predominantly by the acetate fermentation pathway. With increasing depth, there is a shift towards methanogenesis by the CO_2 reduction pathway, as organic matter becomes increasingly recalcitrant, resulting in the depletion of ^{13}C-CH_4 (Hornibrook et al. 2000).

Unfortunately, oxidation and diffusive processes can mask the isotopic signal of methanogenesis, especially in the first meter of the profile (Whiticar 1999; Conrad 2005). CH_4 formed under anaerobic conditions is oxidized during its transport to the soil surface (0–1 m), into surficial oxic layers where bacteria oxidize the ^{12}C-isotope slightly faster than the ^{13}C-isotope, resulting in an increase of the $^{13}C/^{12}C$ ratio of the remaining CH_4. A similar pattern is shown by CH_4 diffusion through a peat profile which also preferentially removes ^{12}C-CH_4 from soil, causing a faster diffusive transport of the lighter isotope ($^{12}CH_4$ with respect to $^{13}CH_4$ and $^{12}CH_3{}^2H$) (Teh et al. 2005; Dorodnikov et al. 2013; Preuss et al. 2013).

Fortunately, differences in $\delta^{13}C$-CH_4 between layers, isotopic fractionation factors of oxidation, and geochemical indications, such as a strong decrease in CH_4 concentrations in the upper profile, serve as indicators to determine to what extent ^{13}C-CH_4 data could be affected by processes like oxidation (De Visscher et al. 2004; Dorodnikov et al. 2013). It is possible to apply a simple model to assess the potential effect of CH_4 oxidation and transport through shifts in $\delta^{13}C$-CH_4 across the soil profile (Dorodnikov et al. 2013). The estimated portion of CH_4 transported and/or oxidized is provided by measuring $\delta^{13}C$-CH_4 of different layers of the profile. The calculation is based on these parameters:

$$F_{tr} = \frac{(\delta_{n+1} - \delta_n)}{10(\alpha_{tr} - 1)} \text{ and } F_{ox} = \frac{(\delta_{n+1} - \delta_n)}{10(\alpha_{ox} - 1)}$$

where F_{tr} and F_{ox} are the estimated potential portion (%) of transported and oxidized CH_4, δ_{n+1} and δ_n are the values of CH_4 in the upper and lower layers, respectively, and α_{tr} and α_{ox} are the isotopic fractionation factors by transport and oxidation. Fractionation during transport process (diffusion) is caused by differences in the diffusion coefficients of isotope species of CH_4 ($^{12}CH_4$, $^{13}CH_4$, and $^{12}CH_3{}^2H$) which differ in molecular weight. A faster diffusive transport of the lighter isotope results in enrichment in the heavier isotope of the remaining gas phase. De Visscher et al. (2004) found that the fractionation factor due to transport (αtr) in landfill-cover soils can be as high as 1.0178, due to the difference in molecular diffusion coefficients of CH_4 isotopes ($\varepsilon \sim 18\%$). Preuss et al. (2013) determined that stable isotope fractionation of CH_4 through water-saturated soils was $\alpha_{diff} = 1.001$, whereas diffusion through soils with air-filled pores was higher, $\alpha_{diff} = 1.013$. Thus, the magnitude of isotope fractionation of molecular diffusion during gas transport is highly influenced by the water content in the soil.

Moreover, CH_4 formed under anaerobic conditions is oxidized to CO_2 during its transport to the soil surface (0–1 m), into the rhizosphere zone, or surficial oxic layers. Bacteria oxidize the ^{12}C-isotope slightly faster than the ^{13}C-isotope; thus, the result is the increase of the $^{13}C/^{12}C$ ratio of the remaining CH_4. Consequently, if CH_4 oxidation occurs, the $\delta^{13}C$ value of the residual CH_4 would become shifted to higher $\delta^{13}C$ values (more enriched than biogenic source) (Chanton et al. 2005). α_{ox} differs widely between sites, ranging from 1.003 to 1.049 as reported by different authors (Bergamaschi 1997; Preuss et al. 2013).

Isotopic differences in organic carbon sources also control the isotopic value of CH_4 and CO_2 gases. Differences in $^{13}C/^{12}C$ ratio of accumulated organic matter in wetland sediments occur as a consequence of photosynthesis. Terrestrial plants can be divided into three major groups based on their photosynthetic pathway: C3, C4, and Crassulacean acid metabolism (CAM). In C3 plants, typical of freshwater aquatic or wetlands environments, CO_2 is fixed during the Calvin cycle yielding C3 compounds as first products and an isotopic signature that varies between − 32 and − 21‰ (Badeck et al. 2005). The effect of the decay processes of organic matter on $\delta^{13}C$ and C/N ratio varies across the soil profile (Khan et al. 2015). The C isotopic composition of the bulk organic matter of deeper layers can deviate gradually from those of the surface because the continual preferential removal of the isotopically lighter molecules from the carbon pool during methanogenesis

results in a progressive shift towards heavier, ^{13}C-enriched values in the residual substrate (Whiticar 1999).

Bacterial oxidation subsequently results in mineralization, which is a process where organic matter is converted into inorganic substances. According to Coleman et al. (1993) and Hackley et al. (1996), CO_2 is isotopically light during the initial aerobic and anaerobic oxidation phases of biodegradation with $\delta^{13}C$ values that vary from −35 to −10‰, covering the range of most terrestrial plants (Clark 2015). The initial input of isotopically light CO_2 associated with earlier biodegradation phases is soon replaced during the methanogenic phase by the constant input of isotopically heavy CO_2 associated to acetate fermentation and microbial CO_2 reduction (the two primary metabolic pathways by which microbial CH_4 is produced). In addition, $\delta^{13}C$-CO_2 data is a complementary tool to discriminate the CO_2 produced as a result of methanogenesis or CH_4 oxidation because they have distinctive values: $\delta^{13}C$-$CO_2 > -10$‰ and $\delta^{13}C$-$CO_2 < -10$‰, respectively (Hackley et al. 1996, 1999).

Results and discussion

Table 1 shows the main characteristics of the soil of the study area. Munsell Soil Chart (wet) indicated black and dark gray colors in most of the layers (e.g., 2.5Y 2.5/1), reflecting anoxic conditions. Observable differences appeared towards the surface where the colors were dark brown (e.g., 10YR 3/1), maybe accompanying the water table oscillations. Gravimetric water content values varied both horizontally and vertically. We observed that the water table depth varied with the island microforms, regulating the saturation level of soils. The values in the center of the island (site C) were higher than in the levee (site A) and surface layers showed a gravimetric water content that increased with depth (~63 to ~76% gravimetric water content in site C vs. ~48 to 69% in site A). Soil texture characterization determined a silty dominant fraction, between 81 and 96%. Clays (smaller than 2 μm) follow in relative abundance with about 10% and the sandy fraction is present in only a 3%. The X-ray diffraction mineral analysis of whole samples indicated the presence of quartz, potassium feldspars, plagioclase, and clays, with a prevalence of the first and last ones. Clay mineralogy analysis for all levels showed the presence of 35–45% of mica-illites, 30–40% of smectites, and 20–25% of kaolinites. The total organic carbon content and the C/N ratio of disturbed soil samples decreased with depth in the three exploratory sites. Total organic carbon varied between 62 and 21 g/kg and showed a C/N ratio between 13.6 and 10.4. $\delta^{13}C$-TOC data obtained from bulk organic matter showed negative values and ranged from −28.8‰, towards the surface, to −24.5‰, in depth. Based on $\delta^{13}C$-TOC, all samples of each core have values of C3 terrestrial plants, just like the C/N values, with a range around 10 to 34 for typical humic substances in terrestrial soils (Khan et al. 2015).

Near-surface CH_4 concentrations ranged from 0.1 on the levee to 93.6 ppm in the center of the island. Soil cores taken in the center of the island from levels 0–30 and 30–60 cm during the first field trip were used to test CH_4 laboratory degassing techniques. Table 2 shows the CH_4 concentrations for different times, using shaking and ultrasonic energy. Three cores were treated for each level and time interval, and a mean CH_4 concentration was calculated. Recovered CH_4 values for the shaking technique were always 1–2 orders of magnitude smaller than those obtained by ultrasonic energy, regardless of the fact that CH_4 concentrations were less at the 0–30 level than at the 30–60 cm. Thus, degassing proved to be more efficient when samples were exposed to ultrasonic energy, yielding higher CH_4 concentrations in a short period of time (5 min/sample) with reproducible results. Therefore, the gas desorption method using ultrasonic energy proved to be a reliable procedure for measuring CH_4 concentrations in sediments of the study area.

The quantification of the CH_4 and CO_2 fluxes carried out with the closed-chamber method at 28 stations distributed regularly on four transects across the whole study area showed an increase from the levee to the center of island (Fig. 2) with variations of 1 order of magnitude for CH_4 fluxes: 0 to 20–30 g/m^2 d. CO_2 fluxes also increased towards the center of the island, with values ranging from 10 g/m^2 d on the levee to 60–80 g/m^2 d, at the center of the island. CH_4 emissions from the study area were similar in magnitude to CH_4 fluxes from natural wetlands (Kayranli et al. 2010). The highest CH_4 fluxes coincided with the near-surface CH_4 anomalies zone detected in the first field trip.

The amount of CH_4 and CO_2 recovered from soil cores (sites C1, C2, and C3) by ultrasonic degassing increased significantly with depth. Figure 3 illustrates the depth distribution of CH_4 and CO_2 concentrations (cores and bags), and the ^{13}C isotopic composition (bags) in relation to others parameters (TOC and $\delta^{13}C$-

Table 1 Characterization of soils. A, levee; B, halfway between A and C; C, center of island. Color of soils: w (wet soils) and d (dry soils); mineralogy of Qtz (quartz), Fd (potassium feldspars), and Pg (plagioclase); TOC, total organic carbon; $\delta^{13}C$ values of TOC were normalized on the L-SVEC-NBS-19 scale (Coplen et al. 2006); w, gravimetric water content

Sample	Color	Qtz %	Fd %	Pg %	Clays %	TOC (g/kg)	$\delta^{13}C$-TOC ± 0.2 (‰)	C/N	Sand %	Silt %	Clay %	w %
C-1 20 cm	10YR 3/1 w; 10YR 5/3 d	48	9	14	30	53.9	− 28.0	13.6	1.3	86.2	12.5	63
C-2 40 cm	2.5Y 2.5/1 w; 10YR 7/2 d	47	8	13	32	47.6	− 27.8	13.2	0.9	86.7	12.5	67
C-3 60 cm	2.5Y 3/1 w 10YR 7/2 d	46	10	12	32	45.1	− 27.0	12.9	0.1	87.4	12.5	69
C-4 80 cm	2.5Y 4/1 w 10YR 7/2 d	46	6	13	36	44.9	− 26.3	12.3	0.5	84.5	15	70
C-5100 cm	2.5Y 5/1 w 10YR 7/2 d	50	11	12	27	34.5	− 26.3	12.4	3.2	91.9	5	75
C-6120 cm	2.5Y 3/1 w 10YR 7/1 d	51	9	13	27	24.7	− 24.8	11.4	1.1	91.5	7.5	76
B-1 20 cm	10YR 3/1 w; 10YR 5/3 d	48	7	14	31	62.6	− 28.8	13.4	1	96.5	2.5	59
B-2 40 cm	10YR 3/1 w; 10YR 5/3 d	46	6	18	31	42.8	− 27.6	13.2	1	89	10	61
B-3 60 cm	2.5Y 2.5/1 w 10YR 7/2 d	53	7	18	24	41.8	− 27.7	12.2	0.5	97	2.5	63
B-4 80 cm	2.5Y 3/1 w 10YR 7/2 d	52	8	14	28	40.1	− 26.4	12.1	1.6	88.5	10	65
B-5100 cm	2.5Y 2.5/1 w 10YR 7/2 d	46	13	11	31	38.8	− 26.1	12.3	0.5	89.5	10	69
B-6120 cm	2.5Y 2.5/1 w 10YR 7/1 d	49	8	15	31	35.5	− 25.6	12.1	0.4	89.6	10	71
A-1 20 cm	10YR 3/2 w; 10YR 5/3 d	54	15	14	19	41.1	− 28.1	12.8	1.2	81.4	17.5	48
A-2 40 cm	10YR 3/3 w; 10YR 5/3 d	55	5	18	23	32.0	− 26.6	11.0	2.4	92.6	5	49
A-3 60 cm	10YR 3/3 w; 10YR 5/3 d	51	8	18	25	28.0	− 26.0	10.5	1.8	90.7	7.5	49
A-4 80 cm	2.5Y 3/1 w 10YR 5/2 d	60	8	11	22	25.5	− 24.5	10.4	1.1	88.9	10	57
A-5100 cm	2.5Y 2.5/1 w 10YR 5/2 d	60	12	12	17	22.6	− 25.7	11.6	2.6	92.4	5	63
A-6120 cm	2.5Y 2.5/1 w 10YR 5/2 d	61	9	15	16	21.7	− 25.3	11.7	3.3	89.2	7.5	69

TOC). The largest concentrations were detected at the 60–90 and 90–120 cm layers. For example, CH_4 overall concentrations (three cores C) increased from ~ 8% at 0–30 cm to ~ 16% at 90–120 cm. CO_2 concentration also increased with depth showing values ranging from ~ 10 to ~ 15%. CH_4 and CO_2 concentrations from bags were less than ~ 10% of the CH_4-CO_2 concentration from core degassing. The concentration of CH_4 dissolved in the pore water also varied with depth (0.00013 to 0.0013 mg/L). The highest concentration of dissolved CH_4 was found in the 90–120 cm depth segment in coincidence with the largest gas volumes from cores. This level corresponds to deep-water saturated layers (with a mean gravimetric water content of ~ 75%) suggesting some influence of water on CH_4 production, especially, related to the achievement of complete anaerobic conditions to produce more gases. In turn, the saturation level regulates the CH_4 subsoil storage mechanism, because the generation of a large amount of gases by decomposition may result in a saturation of pore water, providing the potential for a gas phase to develop as bubbles (Beckwith and Baird 2001). Thus, it is typical to find high concentrations of CH_4 in sediments, rather than in water, due to the low solubility of CH_4 in water. This CH_4 can remain in the sediments due to the sorption capacity of organic-rich

Table 2 Shaking and ultrasonic energy degassing techniques results: CH_4 concentrations ($n = 3$) vs. time

Level of soil	Shaking				Ultrasonic		
	10 min	20 min	30 min	1 h	1 min	2 min	5 min
0–30 cm	81 ± 11 ppmv	1226 ± 76 ppmv	3163 ± 183 ppmv	8190 ± 177 ppmv	2170 ± 156 ppmv	11,336 ± 360 ppmv	51,625 ± 881 ppmv
30–60 cm	257 ± 40 ppmv	3476 ± 102 ppmv	5122 ± 128 ppmv	9371 ± 220 ppmv	4484 ± 216 ppmv	84,361 ± 3315 ppmv	157,580 ± 2249 ppmv

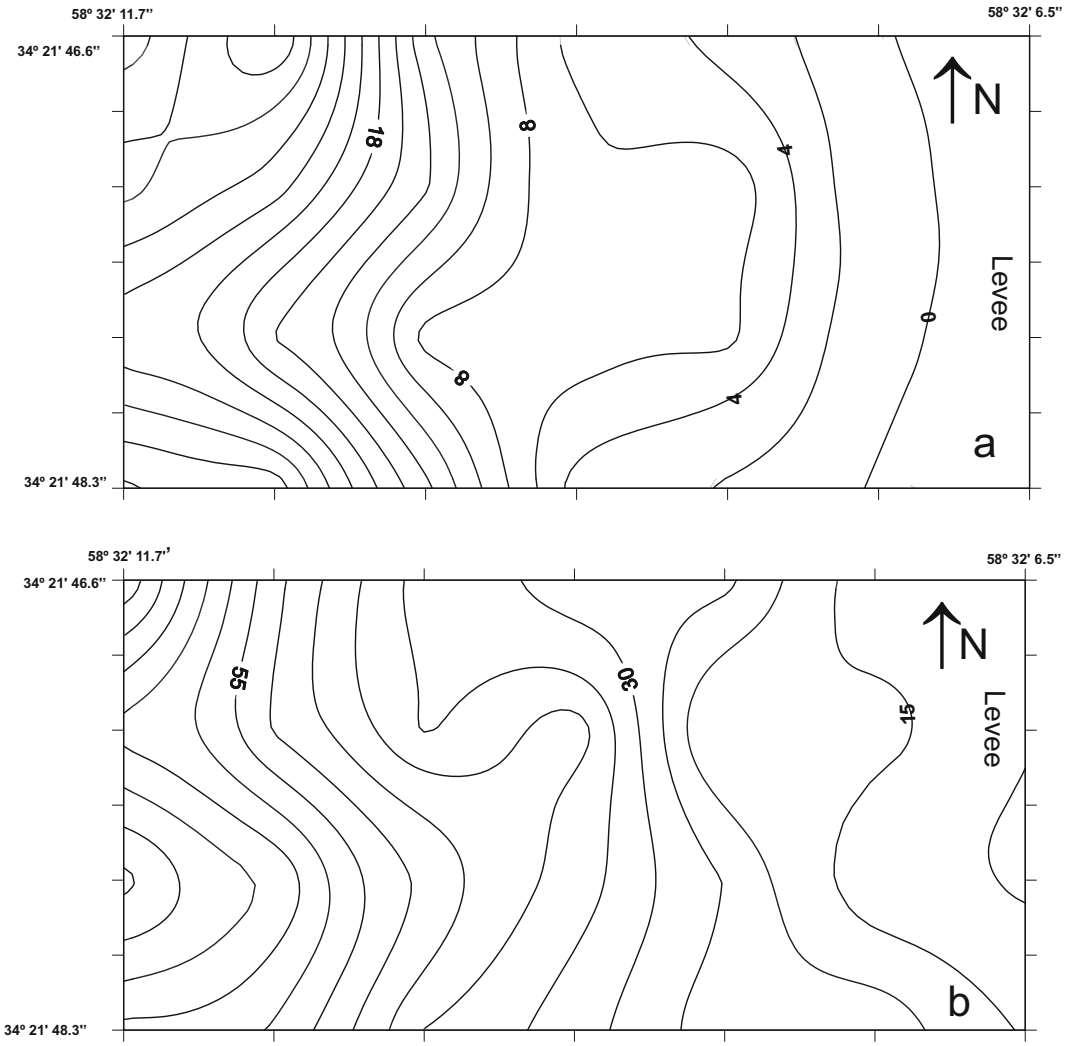

Fig. 2 Sketch showing the increase in closed-chamber CH_4 fluxes (**a**) and CO_2 fluxes (**b**) from the levee to the center of the island. CH_4 flux with CO_2 flux isovalue lines show that CO_2 fluxes were higher than CH_4 fluxes

shales or/and some type of clays, or due to physical limitations on gas transport imposed by the lower gas permeability and higher bulk density of deepest layers compared to surface ones (Teh et al. 2005).

The δ^{13}C-CH_4 data shows a gradual enrichment from the deeper layers to the surface (~ − 71 to ~ − 55‰), whereas the δ^{13}C-TOC varies in the opposite direction (~ − 21 to ~ − 29‰). Moreover, organic matter content decreases as CH_4 and CO_2 increase (Fig. 3). These patterns showed that ^{13}C isotopic composition of bulk organic matter of deeper layers deviates gradually from those of the surface, that is, most chemical and biochemical processes favor the initial incorporation of the lighter isotope in the product, leaving the substrate enriched in the heavy isotope (Werth and Kuzyakov 2010). In addition, this isotopic pattern is consistent with an oxidation process, which was confirmed by a sustained decrease in CH_4 above 90 cm. In particular, the δ^{13}C-CH_4 was approximately − 71 and − 68‰ at 60–120 cm depth, compared to ~ − 62 and − 55‰ at 0–30 cm. On the contrary, the isotopic composition of CO_2 showed more positive values at depth (from ~ − 4‰ at 120 cm to ~ − 23‰ on the surface).

When we evaluated spatial variation (Fig. 4), we observed that CH_4 concentrations in cores from sites A and B were lower than those in the core from site C. CH_4 fluxes measured from closed chambers around sites A, B, and C showed the same pattern with zero values on the levee, and an increase towards the center of the island (0.033 to 11.69 g/m^2 d). We also saw vertical

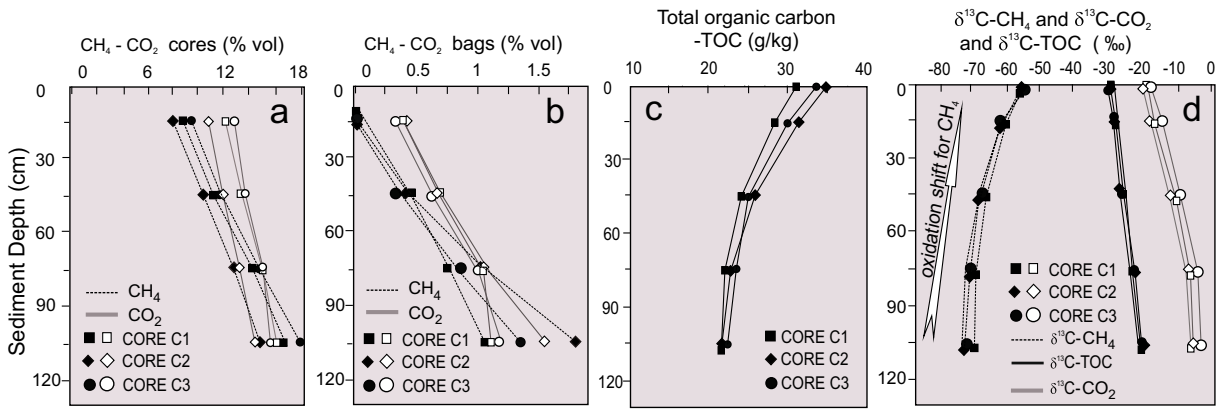

Fig. 3 Results from the three cores sampled in the center of the island during the second field trip. **a**, **b** CH_4 and CO_2 concentrations in cores and bags (note the different scales used and the fact that $CH_4 > CO_2$ only in deepest level); **c** TOC concentration of cores and surface; **d** isotopic values ($\delta^{13}C$-CH_4 and $\delta^{13}C$-CO_2 from bags and CH_4-CO_2 fluxes, and $\delta^{13}C$-TOC of cores and surface)

variations of CH_4 concentrations increasing from ~ 0.1% in the 30–60-cm layer to ~ 1.3% in the 90–120-cm one (core A), and from ~ 4.2% in the 30–60-cm layer to ~ 8.3% in the 90–120-cm one (core B). CH_4 reached ~ 21% at the 90–120-cm level (core C). The lowest CH_4 concentration (~ 0.1%) was found in the surface layer (0–30 cm) of core A, which also showed a low water content (43%). The measurements of gravimetric water content ranged from ~ 60 to ~ 78% in core C vs. ~ 43 to 64% in core A. Also, CH_4 and CO_2 concentrations measured in bags were significantly lower than those in sediments of all cores. The general trend of $\delta^{13}C$-CH_4 was similar to cores sampled in the second field trip, that is, an enrichment of ^{13}C-CH_4 towards the surface, including $\delta^{13}C$-CH_4 fluxes values.

We plotted the $\delta^{13}C$-CH_4 and $\delta^{13}C$-CO_2 values (second and third field trips) on the chart that discriminates the different biogenic sources (Fig. 5) (Whiticar et al. 1986; Coleman et al. 1993). Taking into account that CH_4 production and oxidation also affect the isotopic composition of CO_2 (substrate for methanogenesis as well as a product of CH_4 oxidation), both values were used to identify methanogenesis pathways and oxidation process. The $\delta^{13}C$-CH_4 and $\delta^{13}C$-CO_2 values showed a CO_2 reduction process for the deeper layers (mainly 60–90 and 90–120 cm) with a tendency to

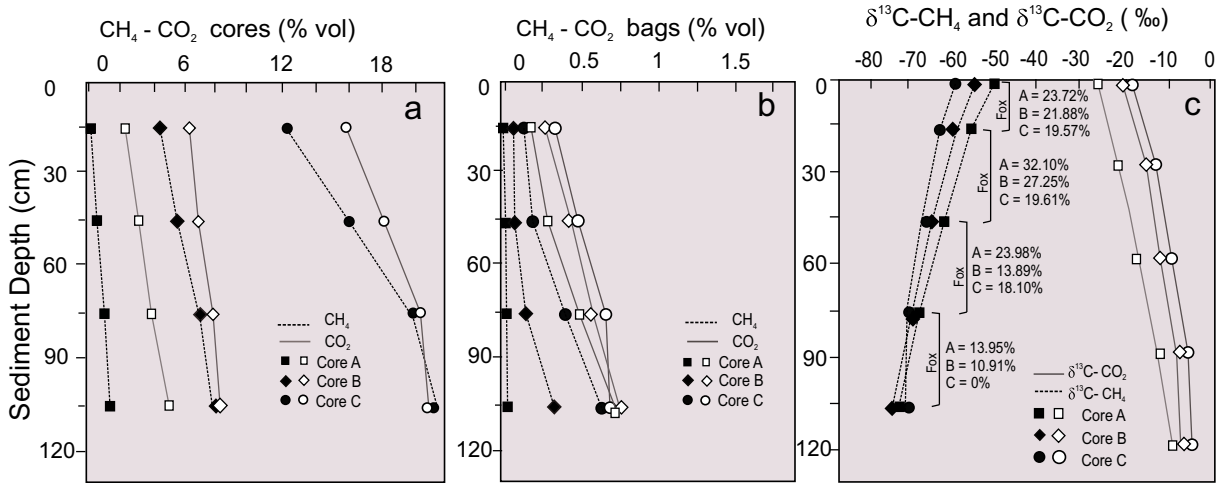

Fig. 4 Results from the three cores sampled during the third field trip. Core A: right beside the levee, core B: about halfway between cores A and C, core C: center of the island. **a**, **b** CH_4 and CO_2 concentrations in cores and bags (note the different scales used and the fact that $CH_4 > CO_2$ only in deepest level); **c** isotopic values, including oxidation fraction percents (Fox)

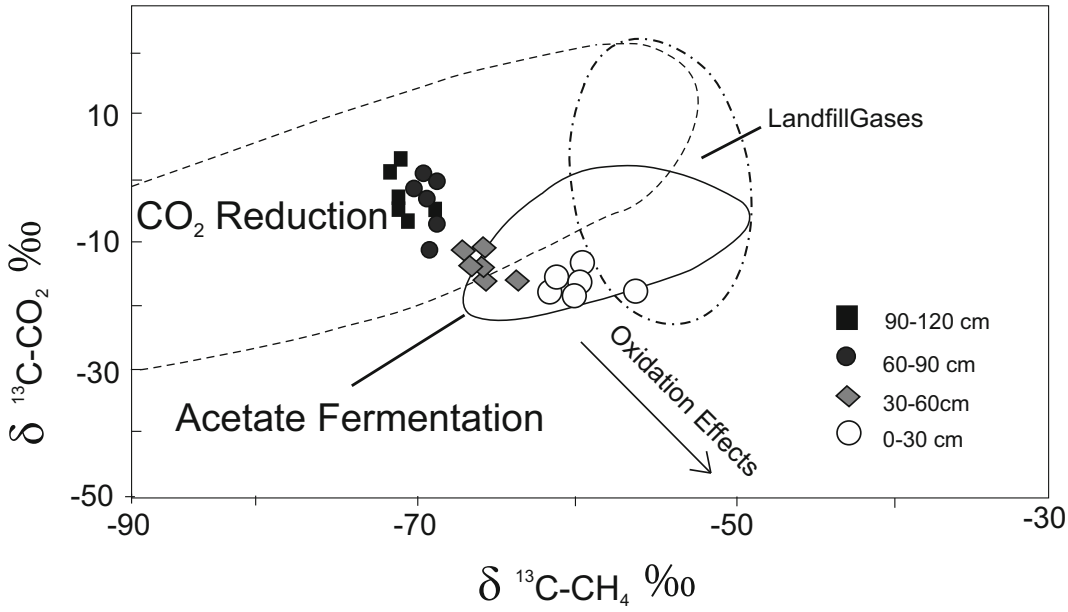

Fig. 5 δ^{13}C-CH_4 and δ^{13}C-CO_2 values from second and third field trips plotted in a chart showing the areas with different biogenic sources (Whiticar et al. 1986; Coleman et al. 1993)

isotopic enrichment of ^{13}C-CH_4 towards more surface layers, and an opposite pattern for ^{13}C-CO_2 values (isotopic depletion). This pattern of δ^{13}C-CH_4 and δ^{13}C-CO_2 across the profile can be the result of changes in the predominance of the type of methanogenic pathway (Hornibrook et al. 2000). Nevertheless, oxidation and/or diffusive processes could be masking the isotopic signal of methanogenesis, especially in the first meter of the profile (Whiticar 1999; Conrad 2005). Thus, based on the changes observed in CH_4 concentrations along the profile, we assumed that there was an oxidation process. Then, the differences of δ^{13}C-CH_4 between layers and the isotopic fractionation factors associated with CH_4 oxidation were used to estimate the CH_4 oxidized fraction, using a $\alpha_{ox} = 1.022$, as cited by Coleman et al. (1981) and Liptay et al. (1998) for methanotrophic microbes.

The estimated oxidation fraction (Fox) for CH_4 reached up to ~32% when we compared isotope values of 0–30 cm layer respect to 30–60 cm level (Fig. 4). Oxidation occurred until a depth of 90 cm, although the calculated oxidized fraction was much smaller (~10%) when we compared isotope values of 60–90 and 90–120 cm levels. We think that at 90–120 cm we are near the CH_4 production zone because it is the only level where CH_4 concentration exceeds CO_2 concentration. So, CH_4 oxidation resulted in a decrease in soil CH_4 concentrations and an enrichment of the residual CH_4 pool in ^{13}C until 90 cm. Similar values were obtained when we calculated the oxidized fraction on the cores from the second field trip, Fig. 3 (~27–28% for above 60 cm and ~10% when we compared isotopic values of 60–90 and 90–120 cm levels). Core A showed the highest oxidized fraction values.

Taking into account the water content of our profiles, we discarded the diffusion process when calculating the transport fraction, since diffusion is significant in drier environments but not in saturated systems (Hapell et al. 1995; Zhang and Krooss 2001). In wetlands, studies about fractionation factors by diffusion (α_{diff}) showed small values, and some authors point out that this process is null in the deeper, more saturated layers (Preuss et al. 2013) or can be present as an estimated transport fraction of around 2–3% (Dorodnikov et al. 2013). Therefore, we assumed that oxidation was the dominant mechanism that affected methanogenic process in our area. The increase in CH_4 concentration, and the shift towards more negative δ^{13}C-CH_4 values with decreasing O_2, suggests that CH_4 production/accumulation became more important than methanotrophy as water content increased. The CH_4/CO_2 ratio did not decrease within the profile because CH_4 and CO_2 production was continuous.

Conclusions

This work combined the study of CH_4 and CO_2 fluxes into atmosphere, and of CH_4 and CO_2 pools, mineralogical, textural, isotopic, and geochemical characterization of subsoil sediments. We focused on the capture of deep gases in saturated soils and we then applied a methodology that allowed us to detect the three fractions: sorbed, free, and dissolved. We described how deep gases (CH_4 and CO_2) are present in the 1.20-m subsoil profile of a site located in an island of the Lower Delta of the Paraná River. Below this depth, sediments become more fluid and this situation would require another CH_4-CO_2 trapping device.

The first results demonstrated an increase in the concentration of both gases (CH_4-CO_2) with depth. The analysis of the vertical profile showed that the concentration of CH_4 trapped in sediments was higher than free CH_4 and dissolved CH_4. Comparison of the total CH_4 with respect to dissolved CH_4 indicated that a significant fraction of CH_4 exists as gas trapped within the sediment column. We identified accumulated CH_4 all along the profile, but the highest concentrations occurred at the 90–120-cm layer. This CH_4 storage capacity of the soil is an important factor in regulating the actual flux rates of CH_4 to the atmosphere. We detected that the places with more soil CH_4 concentration (center of the island) are the places with more CH_4 flux rates.

We saw that the soil above the 90-cm level was the active zone for CH_4 oxidation, resulting in a decrease in soil CH_4 concentrations and enrichment in ^{13}C of the residual CH_4 pool. In this segment, CH_4 concentrations are the result of both production and oxidation processes. Accumulation of CH_4 is probably accounted by the physical limitations in gas transport imposed by the lower gas permeability in the levels with high gravimetric water content. Also, some mechanism of CH_4 sorption is occurring in the sediments, as shown by the high CH_4 concentrations obtained from cores using an ultrasonic degassing technique, which was more efficient than the shaking procedure. Smectites clays were detected all across the profile.

CH_4 oxidation appeared to control CH_4 emissions because CH_4 emitted from land was significantly enriched in ^{13}C when compared to ^{13}C from CH_4 of the 90–120-cm depth. In this way, stable isotope data provided great information, attributing CH_4 and CO_2 gases to CO_2 reduction production and consumption processes. The mechanism through which CH_4 was oxidized to CO_2 before the gases reached the soil surface is also supported by $\delta^{13}C$-CO_2 values (associated to $\delta^{13}C$-CH_4) of the different depths of the column. $\delta^{13}C$ isotopes of terrestrial organic carbon in the profile also responded to CH_4-CO_2 production because, as the process of methanogenesis progresses, consuming organic matter, the signal of the residual $\delta^{13}C$-TOC shifts to more enriched values.

Acknowledgments The authors are grateful to Stable Isotopes Laboratory staff members, Liliana Marban, Estela Ducos, Fernanda Cravero and Gabriel Giordarengo.

Funding information This research was supported by the Instituto de Geocronología y Geología Isotópica (UBA-CONICET).

References

Aravena, R., Warner, B. G., Charman, D. J., Belyea, L. R., Mathur, S. P., & Dinel, H. (1993). Carbon isotopic composition of deep carbon gases in an ombrogeneous peatland, northwestern Ontario, Canada. *Radiocarbon, 35*, 271–276. https://doi.org/10.1017/S0033822200014016.

Badeck, F. W., Tcherkez, G., Nogués, S., Piel, C., & Ghashghaie, J. (2005). Post-photosynthetic fractionation of stable carbon isotopes between plant organs—a widespread phenomenon. *Rapid Communications in Mass Spectrometry, 19*, 1381–1391. https://doi.org/10.1002/rcm.1912.

Baird, A. J., Beckwith, C. W., Waldron, S., & Waddington, J. M. (2004). Ebullition of methanecontaining gas bubbles from near surface Sphagnum peat. *Geophysical Research Letters, 31*, L21505. https://doi.org/10.1029/2004GL021157.

Beckwith, C. W., & Baird, A. J. (2001). Effect of biogenic gas bubbles on water flow through poorly decomposed blanket peat. *Water Resources Research, 37*(3), 551–558.

Bergamaschi, P. (1997). Seasonal Variation of Stable Hydrogen and Carbon Isotope Ratios in Methane from a Chinese Rice Paddy. *Journal of Geophysical Research, 102*(D21), 25,383–25,393. https://doi.org/10.1029/97JD01664.

Bernard, B. B., Brooks, J. M., & Sackett, W. M. (1978). Light hydrocarbons in recent Texas continental shelf and slope sediments. *Journal of Geophysical Research, 83*, 4053. https://doi.org/10.1029/JC083iC08p04053.

Biscaye, P. E. (1965). Mineralogy and sedimentation of recent deep-sea clay in the Atlantic Ocean and adjacent seas and oceans. *Bulletin Geological Society of America, 76*, 803. https://doi.org/10.1130/0016-7606(1965)76[803:MASORD]2.0.CO;2.

Bridgham, S. D., Cadillo-Quiroz, H., Keller, J. K., & Zhuang, Q. (2013). Methane emissions from wetlands: biogeochemical, microbial, and modeling perspectives from local to global scales. *Global Change Biology, 19*, 1325–1346. https://doi.org/10.1111/gcb.12131.

Chanton, J. P. (2005). The Effect of Gas Transport on the Isotope Signature of Methane in Wetlands. *Organic Geochemistry, 36*, 753–768. https://doi.org/10.1016/j.orggeochem.2004.10.007.

Chanton, J. P., Martens, C. S., & Kelley, C. A. (1989). Gas transport from methane-saturated tidal fresh-water and wetland sediments. *Limnology and Oceanography, 34*, 807–819. https://doi.org/10.4319/lo.1989.34.5.0807.

Clark. (2015). *Groundwater geochemistry and isotopes*. Boca Raton, Florida: CRC Press.

Coleman, D. D., Risatti, J. B., & Schoell, M. (1981). Fractionation of Carbon and Hydrogen Isotopes by Methane-Oxidizing Bacteria. *Geochimica et Cosmochimica Acta, 45*, 1033–1037. https://doi.org/10.1016/0016-7037(81)90129-0.

Coleman D. D., Liu, C. L., Hackley, K. C. & Benson, L. J. (1993). *Identification of Landfill Methane Using Carbon and Hydrogen Isotope Analysis*. Proceedings of 16th International Madison Waste Conference, Municipal & Industrial Waste (pp. 303–314). Madison: Department of Engineering Professional Development, University of Wisconsin, 22-23 September.

Comas, X., Slater, L., & Reeve, A. (2005). Spatial Variability in Biogenic Gas Accumulations in Peat Soils Is Revealed by Ground Penetrating Radar (GPR). *Geophysical Research Letters, 32*, L08401. https://doi.org/10.1029/2004gl022297.

Comas, X., Kettridge, N., Binley, A., Slater, L., Parsekian, A., Baird, A. J., Strack, M., & Waddington, J. M. (2014). The effect of peat structure on the spatial distribution of biogenic gases within bogs. *Hydrological Processes, 28*, 5483–5494. https://doi.org/10.1002/hyp.10056.

Conrad, R. (2005). Quantification of methanogenic pathways using stable carbon isotopic signatures: a review and a proposal. *Organic Geochemistry, 36*, 739–752. https://doi.org/10.1016/j.orggeochem.2004.09.006.

Coplen, T. B., Brand, W. A., Gehre, M., Gröning, M., Meijer, H. A. J., Toman, B., & Verkouteren, R. M. (2006). New guidelines for δ13C measurements. *Analytical Chemistry, 78*, 2439–2441. https://doi.org/10.1021/ac052027c.

Coulthard, T. J., Baird, A. J., Ramirez, J., & Waddington, J. M. (2009). Methane dynamics in peat: importance of shallow peats and a novel reduced-complexity approach for modeling ebullition. In A. J. Baird, L. R. Belyea, X. Comas, A. S. Reeve, & L. D. Slater (Eds.), *Carbon cycling in northern peatlands* (pp. 173–185). Washington DC: American Geophysical Union.

Couwenberg, J., Dommain, R., & Joosten, H. (2010). Greenhouse gas fluxes from tropical peatlands in south-east Asia. *Global Change Biology, 16*, 1715–1732. https://doi.org/10.1111/j.1365-2486.2009.02016.x.

De Visscher, A., De Pourcq, I., & Chanton, J. (2004). Isotope Fractionation Effects by Diffusion and Methane Oxidation in Landfill Cover Soils. *Journal of Geophysical Research, 109*, D18111. https://doi.org/10.1029/2004jd004857.

Dorodnikov, M., Marushchak, M., Biasi, C., & Wilmking, M. (2013). Effect of microtopography on isotopic composition of methane in porewater and efflux at a boreal peatland. *Boreal Environment Research, 18*, 269–279.

EPA (2001). Wetlands Classification and Types. Resource document. Environmental Protection Agency of United States, Office of Water EPA 843-F-01-002b, Oceans and Watersheds (4502T). http://water.epa.gov/type/wetlands/types_index.cfm

Gal'chenko, V. F., Lein, A., & Ivanov, M. V. (2004). Methane content in the bottom sediments and water column of the Black Sea. *Microbiology, 73*(2), 211–223.

Garnett, M. H., Hardie, S. M. L., & Murray, C. (2011). Radiocarbon and stable carbon analysis of dissolved methane and carbon dioxide from the profile of a raised peat bog. *Radiocarbon, 53*, 71–83. https://doi.org/10.1017/S0033822200034366.

Glaser, P. H., Chanton, J. P., Morin, P., Rosenberry, D. O., Siegel, D. I., Ruud, O., Chasar, L. I., & Reeve, A. S. (2004). Surface Deformations as Indicators of Deep Ebullition Fluxes in a Large Northern Peatland. *Global Biogeochemical Cycles, 18*, GB1003. https://doi.org/10.1029/2003gb002069.

Hackley, K. C., Coleman, D. D., & Liu, C. L. (1996). Environmental isotope characteristics of landfill leachates and gases. *Groundwater, 34*, 827–836. https://doi.org/10.1111/j.1745-6584.1996.tb02077.x.

Hackley, K. C., Liua, C. L., & Trainorb, D. (1999). Isotopic identification of the source of methane in subsurface sediments of an area surrounded by waste disposal facilities. *Applied Geochemistry, 14*, 119–131. https://doi.org/10.1016/S0883-2927(98)00036-5.

Hapell, J. D., Chanton, J. P., & Showers, W. J. (1995). Methane transfer across the water-air interface in stagnant wooded swamps of Florida: evaluation of mass transfer coefficients and isotopic fractionation. *Limnology and Oceanography, 40*, 290–298.

Hornibrook, E. R. C., Longstaffe, W. S., & Fyfe, W. S. (1997). Spatial distribution of microbial methane production pathways in temperate zone wetland soils: stable carbon and hydrogen isotope evidence. *Geochimica et Cosmochimica Acta, 61*, 745–753.

Hornibrook, E. R. C., Longstaffe, F. J., & Fyfe, W. S. (2000). Evolution of stable carbon isotope compositions for methane and carbon dioxide in freshwater wetlands and other anaerobic environments. *Geochimica et Cosmochimica Acta, 64*, 1013–1027.

INTA. (1990). *Atlas de Suelos de la República Argentina*. Buenos Aires: Instituto de Suelos-INTA.

Kandus, P., Quintana, R. D., & Bó, R. F. (2006). *Patrones de Paisaje y Biodiversidad del Bajo Delta del Río Paraná. Mapa de Ambientes*. Buenos Aires: Pablo Casamajor.

Kayranli, B., Scholz, M., Mustafa, A., & Hedmark, A. (2010). Carbon storage and fluxes within freshwater wetlands: a critical review. *Wetlands, 30*, 111–124. https://doi.org/10.1007/s13157-009-0003-4.

Khalil, M. (2000). Atmospheric methane: an introduction. In M. A. K. Khalil (Ed.), *Atmospheric methane. Its role in the global environment* (pp. 1–8). New York: Springer.

Khan, N. S., Vane, C. H., & Horton, B. P. (2015). Stable carbon isotope and C/N geochemistry of coastal wetland sediments as sea-level indicator. In I. Shennan, A. J. Long, & B. P. Horton (Eds.), *Handbook of sea-level research* (pp. 295–311). New Jersey: John Wiley & Sons Ltd..

Lai, D. Y. (2009). Methane dynamics in northern peatlands: a review. *Pedosphere, 19*, 409–421. https://doi.org/10.1016/S1002-0160(09)00003-4.

Le Mer, J., & Roger, P. (2001). Production, oxidation, emission and consumption of methane by soils: a review. *European Journal of Soil Biology, 37*, 25–50. https://doi.org/10.1016/S1164-5563(01)01067-6.

Liptay, K., Chanton, J., Czepiel, P., & Mosher, B. (1998). Use of stable isotopes to determine methane oxidation in landfill cover soils. *Journal of Geophysical Research, 103*, 8243–8250. https://doi.org/10.1029/97JD02630.

Magen, C., Lapham, L., Pohlman, J. W., Marshall, K., Bosman, S., Casso, M., & Chanton, J. P. (2014). A simple headspace equilibration method for measuring dissolved methane. *Limnology and Oceanography: Methods, 12*, 637–650. https://doi.org/10.4319/lom.2014.12.637.

Malvárez, A. I. (1997). Las comunidades vegetales del Delta del río Paraná. Su relación con factores ambientales y patrones de paisaje. Tesis Doctoral. Universidad de Buenos Aires. Argentina.

Martens, C. S., Kelley, C. A., Chanton, J. P., & Showers, W. J. (1992). Carbon and hydrogen isotopic characterization of methane from wetlands and lakes of the Yukon-Kuskokwim delta, western Alaska. *Journal of Geophysical Research, 97*, 16689. https://doi.org/10.1029/91JD02885.

Medina, R. A., & Codignotto, J. O. (2013). Evolución del delta del río Paraná y su posible vinculación con el calentamiento global. *Revista Museo Argentino Ciencias Naturales, 15*(2), 191–200.

Preuss, I., Knoblauch, C., Gebert, J., & Pfeiffer, E. M. (2013). Improved quantification of microbial CH_4 oxidation efficiency in arctic wetland soils using carbon isotope fractionation. *Biogeosciences, 10, 2539–2552*. https://doi.org/10.5194/bg-10-2539-2013.

Ramirez, J. A., Baird, A. J., Coulthard, T. J., & Waddington, J. M. (2015). Ebullition of methane from peatlands: does peat act as a signal shredder? *Geophysical Research Letters, 42*, 3371–3379. https://doi.org/10.1002/2015GL063469.

Rosenberry, D. O., Glaser, P. H., & Siegel, D. I. (2006). The hydrology of northern peatlands as affected by biogenic gas: current developments and research needs. *Hydrological Processes, 20*, 3601–3610. https://doi.org/10.1002/hyp.6377.

Sanci, R., & Panarello, H. O. (2016). Carbon stable isotopes as indicators of the origin and evolution of CO2 and CH4 in urban solid waste disposal sites and nearby áreas. *Environmental Earth Sciences, 75*, 294. https://doi.org/10.1007/s12665-015-4906-5.

Sanci, R., Panarello, H., & Ostera, H. (2012). CO_2 emissions from a municipal site for final disposal of solid waste in Gualeguaychú, Entre Ríos Province, Argentina. *Environmental Earth Sciences, 66*, 519–528. https://doi.org/10.1007/s12665-011-1260-0.

Schmitt, M., Faber, E., Botz, R., & Stoffers, P. (1991). Extraction of methane from seawater using ultrasonic vacuum degassing. *Analytical Chemistry, 63*(5), 529–532.

Schumacher, B. A. (2002). *Methods for the determination of total organic carbon (TOC) in soils and sediments*. Resource document, United States Environmental Protection Agency, NCEA-C- 1282 EMASC-001. http://bcodata.whoi.edu/LaurentianGreatLakes_Chemistry/bs116.pdf. Accessed 21 Feb 2014

Scranton, M. I., Donaghay, P., & Sieburth, J. M. (1995). Nocturnal methane accumulation in the pycnocline of an anoxic estuarine basin. *Limnology and Oceanography, 40*, 666–672. https://doi.org/10.4319/lo.1995.40.4.0666.

Steinmann, P., Eilrich, B., Leuenberger, M., & Burns, S. J. (2008). Stable carbon isotope composition and concentrations of CO_2 and CH_4 in the deep catotelm of a peat bog. *Geochimica et Cosmochimica Acta, 72*, 6015–6026. https://doi.org/10.1016/j.gca.2008.09.024.

Strack, M., Waddington, J. M., & Tuittila, E. S. (2004). Effect of water table drawdown on northern peatland methane dynamics: implications for climate change. *Global Biogeochemical Cycles, 18*, GB4003. https://doi.org/10.1029/2003GB002209.

Strack, M., Kellner, E., & Waddington, J. M. (2005). Dynamics of Biogenic Gas Bubbles in Peat and Their Effects on Surface Deformations as Indicators of Deep Ebullition Fluxes in a Large Northern Peatland. *Global Biogeochemical Cycles, 19*, GB1003. https://doi.org/10.1029/2004GB002330.

Teh, Y. A., Silver, W. L., & Conrad, M. E. (2005). Oxygen effects on methane production and oxidation in humid tropical forest soils. *Global Change Biology, 11*, 1283–1297. https://doi.org/10.1111/j.1365-2486.2005.00983.x.

Waldron, S., Hall, A. J., & Fallick, A. E. (1999). Enigmatic stable isotope dynamics of deep peat methane. *Global Biogeochemical Cycles, 13*, 93–100. https://doi.org/10.1029/1998GB900002.

Wassmann, R., Neue, H. U., Alberto, M. C. R., Lantin, R. S., Bueno, C., Llenaresas, D., Arah, J. R. M., Papen, H., Seiler, W., & Rennenberg, H. (1996). Fluxes and Pools of Methane in Wetlands Rices Oils with Varying Organic Inputs. *Environmental Monitoring and Assessment, 42*, 163–173. https://doi.org/10.1007/BF00394048.

Werth, M., & Kuzyakov, Y. (2010). ^{13}C fractionation at the root–microorganisms–soil interface: a review and outlook for partitioning studies. *Soil Biology and Biochemistry, 42*, 1372–1384. https://doi.org/10.1016/j.soilbio.2010.04.009.

Whalen, S. C. (2005). Biogeochemistry of methane exchange between natural wetlands and the atmosphere. *Environmental Engineering Science, 22*, 73–94. https://doi.org/10.1089/ees.2005.22.73.

Whiticar, M. J. (1999). Carbon and hydrogen isotope systematics of bacterial formation and oxidation of methane. *Chemical Geology, 161*, 291–314. https://doi.org/10.1016/S0009-2541(99)00092-3.

Whiticar, M. J., Faber, E., & Schoell, M. (1986). Biogenic methane formation in marine and freshwater environments: CO_2 reduction vs. acetate fermentation—isotope evidence. *Geochemica et Cosmochimica Acta, 50*, 693–709.

Wuebbles, D. J., & Hayhoe, K. (2002). Atmospheric methane and global change. *Earth-Science Reviews, 57*, 177–210. https://doi.org/10.1016/S0012-8252(01)00062-9.

Zhang, T., & Krooss, B. M. (2001). Experimental investigation on the carbon isotope fractionation of methane during gas migration by diffusion through sedimentary rocks at elevated temperature and pressure. *Geochemica et Cosmochimica Acta, 65*, 2723–2742.